

This item is the archived peer-reviewed author-version of:

Comparing temperature data sources for use in species distribution models : from in-situ logging to remote sensing

Reference:

Lembrechts Jonas, Lenoir Jonathan, Roth Nina, Hattab Tarek, Milbau Ann, Haider Sylvia, Pellissier Loïc, Pauchard Anibal, Backes Amanda Ratier, Dimarco Romina D.,- Comparing temperature data sources for use in species distribution models : from in-situ logging to remote sensing
Global ecology and biogeography - ISSN 1466-822X - Hoboken, Wiley, 2019, 19 p.
Full text (Publisher's DOI): <https://doi.org/10.1111/GEB.12974>
To cite this reference: <https://hdl.handle.net/10067/1615630151162165141>

1 **Comparing temperature data sources for use in species distribution models:**
2 **from *in-situ* logging to remote sensing**

3 ***Running header: temperature data for distribution models***

4 Jonas J. Lembrechts^{1,*}, Jonathan Lenoir², Nina Roth³, Tarek Hattab^{4,2}, Ann Milbau⁵, Sylvia
5 Haider^{6,7}, Loïc Pellissier^{8,9}, Aníbal Pauchard^{10,11}, Amanda Ratier Backes^{6,7}, Romina. D.
6 Dimarco¹², Martin A. Nuñez¹³, Juha Aalto^{14,15}, Ivan Nijs¹

7 ¹ Centre of Excellence Plants and Ecosystems (PLECO), University of Antwerp, 2610 Wilrijk,
8 Belgium

9 ² UR “Ecologie et Dynamique des Systèmes Anthropisés” (EDYSAN, UMR 7058 CNRS-
10 UPJV), Université de Picardie Jules Verne, 1 Rue des Louvels, 80037 Amiens Cedex 1,
11 France

12 ³ Biogeography and Geomatics, Department of Physical Geography, Stockholm University,
13 10691 Stockholm, Sweden

14 ⁴ MARBEC (IRD, Ifremer, Université de Montpellier, CNRS), Sète Cedex, France

15 ⁵ Research Institute for Nature and Forest - INBO, Havenlaan 88, bus 73, 1000 Brussels,
16 Belgium

17 ⁶ Institute of Biology / Geobotany and Botanical Garden, Martin Luther University Halle-
18 Wittenberg, Halle (Saale), Germany

19 ⁷ German Centre for Integrative Biodiversity Research (iDiv) Halle-Jena-Leipzig, Leipzig,
20 Germany

21 ⁸ Landscape Ecology, Institute of Terrestrial Ecosystems, ETH Zürich, CH-8092 Zürich,
22 Switzerland

23 ⁹ Swiss Federal Research Institute WSL, CH-8903 Birmensdorf, Switzerland

24 ¹⁰ Laboratorio de Invasiones Biológicas, Facultad de Ciencias Forestales, Universidad de
25 Concepción, Casilla 160-C, 4030000 Concepción, Chile

26 ¹¹ Institute of Ecology and Biodiversity (IEB), 8320000 Santiago, Chile

27 ¹² Grupo de Ecología de Poblaciones de Insectos, INTA-CONICET, Modesta Victoria 4450,
28 8400, Bariloche, Argentina

29 ¹³ Grupo de Ecología de Invasiones, INIBIOMA, CONICET-Universidad Nacional del
30 Comahue, Av. de Los Pioneros 2350, 8400 Bariloche, Argentina

31 ¹⁴ Dept of Geosciences and Geography, Gustaf Hällströmin katu 2a, FIN-00014 Univ. of
32 Helsinki, Finland

33 ¹⁵ Finnish Meteorological Inst., Finland

34 *Corresponding author: jonas.lembrechts@uantwerpen.be, +3232651727.

35 Orcid ID JJL: orcid.org/0000-0002-1933-0750.

36 Orcid ID JL: orcid.org/0000-0003-0638-9582.

37 Orcid ID TH: orcid.org/0000-0002-1420-5758.

38 Orcid ID AM: orcid.org/0000-0003-3555-8883.

39 Orcid ID SH: orcid.org/0000-0002-2966-0534.

40 Orcid ID AP: orcid.org/0000-0003-1284-3163.

41 *Orcid ID JA: orcid.org/0000-0001-6819-4911*

42

43

44 **Acknowledgements**

45 The research leading to this publication has received funding from the Research Foundation-

46 Flanders (FWO) through a personal grant to JJL, from the European INTERACT-program

47 through a Transnational Access grant to JJL and through the Methusalem funding of the

48 Flemish Community through the Research Council of the University of Antwerp.

49 Computational resources and services were provided where needed by the HPC core facility

50 CalcUA of the University of Antwerp, and VSC (Flemish Supercomputer Center), funded by

51 the Research Foundation - Flanders (FWO) and the Flemish Government – department EWI.

52 AP funded by CONICYT PFB-23 and Fondecyt 1180205. The authors declare no conflicts of

53 interest.

54 **Biosketch**

55 This study is performed in the framework of (1) the Mountain Invasion Research Network

56 (MIREN, www.mountaininvasions.org), a global consortium of plant ecologists focussing on

57 species redistributions in mountain regions, and (2) SoilTemp (<https://soiltemp.weebly.com>),

58 a global effort to create a database of in-situ soil temperature measurements for use in

59 ecology.

60

61

62

63

64 **Abstract**

65 **Aim:** While species distribution models (SDMs) traditionally link species occurrences to free-
66 air temperature data at coarse spatiotemporal resolution, the distribution of organisms might
67 rather be driven by temperatures more proximal to their habitats. Several solutions are
68 currently available, such as downscaled or interpolated coarse-grained free-air temperatures,
69 satellite-measured land surface temperatures (LST) or *in-situ* measured soil temperatures. A
70 comprehensive comparison of temperature data sources and their performance in SDMs is
71 however currently lacking.

72 **Location:** Northern Scandinavia

73 **Time period:** 1970 - 2017

74 **Major taxa studied:** Higher plants

75 **Methods:** We evaluated different sources of temperature data (WorldClim, CHELSA,
76 MODIS, E-OBS, topoclimate and soil temperature from miniature data loggers), differing in
77 spatial resolution (1'' to 0.1°), measurement focus (free-air, ground-surface or soil
78 temperature) and temporal extent (year-long vs. long-term averages), and use them to fit
79 SDMs for 50 plant species with different growth forms in a high-latitudinal mountain region.

80 **Results:** Differences between these temperature data sources originating from measurement
81 focus and temporal extent overshadow the effects of temporal climatic differences and
82 spatiotemporal resolution, with elevational lapse rates ranging from -0.6 °C per 100 m for
83 long-term free-air temperature data to -0.2 °C per 100 m for in-situ soil temperatures. Most
84 importantly, we found that the performance of the temperature data in SDMs depended on
85 species' growth forms. The use of in-situ soil temperatures improved the explanatory power

86 of our SDMS (R^2 on average +16%), especially for forbs and graminoids (R^2 : +24% and
87 +21% on average, respectively) compared to the other data sources.

88 **Main conclusions:** We suggest future studies using SDMs to use the temperature dataset that
89 best reflects the species' ecology, rather than automatically using coarse-grained data from
90 WorldClim or CHELSA.

91

92 **Keywords:** bioclimatic variables, climate change, growth forms, microclimate, mountains,
93 land surface temperature, bioclimatic envelope modelling, soil temperature, species
94 distribution modelling

95 **Introduction**

96 Species distribution models (SDMs) are widely used to describe and forecast the spatial
97 distribution of species (Elith & Leathwick, 2009). SDMs relate species occurrence data with
98 information about the environmental conditions at these locations (Guisan & Thuiller, 2007;
99 Elith & Leathwick, 2009; Jiménez-Valverde *et al.*, 2011). The most common strategy is to
100 work with long-term (e.g. 30 years) interpolated averages of a set of bioclimatic variables at
101 30'' resolution (ca. 1×1 km at the equator), e.g. WorldClim or CHELSA (Hijmans *et al.*,
102 2005; Warren *et al.*, 2008; Sears *et al.*, 2011; Slavich *et al.*, 2014; Gonzalez-Moreno *et al.*,
103 2015; Karger *et al.*, 2017). While such macroclimate data might be sufficient to capture the
104 conditions on flat terrains, many environments host a heterogeneous topography (e.g. across
105 steep elevational gradients in mountain regions) that make the microclimate near the ground
106 vary noticeably over short distances (Gottfried *et al.*, 1999; Holden *et al.*, 2011; Scherrer &
107 Körner, 2011; Sears *et al.*, 2011; Opedal *et al.*, 2015; Stewart *et al.*, 2018). In order to make
108 realistic forecasts of species distributions and distribution shifts in such heterogeneous
109 environments, it has been suggested that climate data at finer spatiotemporal resolutions are
110 needed (Illan *et al.*, 2010; Scherrer & Körner, 2011; Graae *et al.*, 2012; Lenoir *et al.*, 2013;
111 Opedal *et al.*, 2015; Graae *et al.*, 2018). Such new climate datasets including *in-situ* logging
112 and remote sensing are now increasingly becoming available (Bramer *et al.*, 2018). Yet, an
113 evaluation of their performance in species distribution models is necessary to provide
114 guidance for future studies, in particular those predicting species responses to climate change
115 (Stewart *et al.*, 2018).

116 In the high-latitude and high-elevation areas of northern Europe, local temperatures have been
117 found to vary up to 6° C within 1 km^2 spatial units, reflecting the local topography (Lenoir *et*
118 *al.*, 2013). This high temperature variation depends for instance on the interaction between
119 temperature and snow distribution, and consequently affects the length of the local growing

120 season (Körner, 2003; Aalto *et al.*, 2018). Local temperatures also vary strongly between
121 seasons, and short-term extreme weather conditions have been shown to be more relevant for
122 species distributions than the average climatic conditions (Ashcroft & Gollan, 2012).
123 Including this variation into SDMs is likely to be crucial, for instance in the context of
124 stepping stones, holdouts or microrefugia (Dobrowski, 2011; Opedal *et al.*, 2015; Meineri &
125 Hylander, 2017). Stepping stones refer to areas with microclimates that facilitate species'
126 range shifts, e.g. upward or poleward movement during climate change or after non-native
127 species introductions (Pauchard *et al.*, 2009; Hannah *et al.*, 2014; Lembrechts *et al.*, 2017).
128 Holdouts and microrefugia on the other hand are areas with a relatively stable microclimate
129 where isolated populations can persist for a certain time (Ashcroft, 2010; Hannah *et al.*, 2014;
130 Lenoir *et al.*, 2017; Meineri & Hylander, 2017). Climatic variability within an area can indeed
131 considerably buffer climate warming effects (Lenoir *et al.*, 2013; Lenoir *et al.*, 2017), which
132 often remains undetected using macroclimate data, possibly leading to the overestimation of
133 rates of extinction and range expansion (Willis & Bhagwat, 2009).

134 Moreover, many organisms (particularly small-stature plants, certain types of insects and soil
135 microbes) experience temperatures at ground or sub-surface level, which can differ strongly
136 from ambient air temperatures that are usually measured at 2 m above the soil surface (Poorter
137 *et al.*, 2016; Aalto *et al.*, 2018; Körner & Hiltbrunner, 2018). Especially in high-latitude and
138 high-elevation regions, snow cover for example acts as an insulator, thereby strongly
139 decoupling soil and air temperatures (Pauli *et al.*, 2013; Poorter *et al.*, 2016; Thompson *et al.*,
140 2018), while biophysical processes due to vegetation cover may also decouple upper
141 atmospheric conditions from boundary layer conditions (Geiger, 1950).

142 In order to overcome this spatiotemporal mismatch between climate data and species ecology
143 and to improve predictions of species' current and future distributions, four main approaches
144 are commonly used: (i) to downscale existing coarse-grained (i.e. 1000 x 1000 m resolution)

145 climate data (McCullough *et al.*, 2016); (ii) to interpolate climate station data (Aalto *et al.*,
146 2017), (iii) to gather local climate data through field measurements (Potter *et al.*, 2013;
147 Slavich *et al.*, 2014; Lenoir *et al.*, 2017); or (iv) to monitor climatic conditions continuously
148 in space and time through remote sensing technologies (e.g. satellite-measured land surface
149 temperatures) (Wan, 2008; Metz *et al.*, 2014; Neteler *et al.*, 2014). In the first two approaches,
150 a high spatial resolution can be obtained using topographic variables derived from digital
151 elevation models which are available at much finer resolutions (e.g. 1'', which is about 30 ×
152 30 m at the equator). Such downscaled or interpolated climate data has been found to be a
153 significant improvement over macroclimatic variables for modelling species distributions
154 (Randin *et al.*, 2009b; Dobrowski, 2011; Slavich *et al.*, 2014; Meineri & Hylander, 2017).

155 In the third approach, one uses actual *in-situ* measurements to provide fine-grained climatic
156 conditions with high spatial accuracy (microclimate) (Opedal *et al.*, 2015; Meineri &
157 Hylander, 2017). Such field measurements can also be interpolated to the level of regional
158 climate using topographical information (Ashcroft *et al.*, 2008; Maclean *et al.*, 2017; Greiser
159 *et al.*, 2018), yet usually cover short temporal and small geographical extents only. In addition
160 to a fine spatial resolution, *in-situ* measurements provide the opportunity to adapt the
161 measurement focus to the ecology or life form of the species, e.g. by measuring near-surface
162 soil temperature instead of air temperature. Gathering *in-situ* temperature data, however,
163 requires considerably more resources than the previously mentioned downscaling approaches
164 (Opedal *et al.*, 2015; Meineri & Hylander, 2017). Increasing the spatiotemporal resolution and
165 extent of such field measurements generally refines the predictions, but also presents a
166 logistical challenge (Wundram *et al.*, 2010; Meineri & Hylander, 2017).

167 Finally, the fourth approach, i.e. using remotely sensed data, is now more frequently used in
168 SDMs (Pottier *et al.*, 2014), for instance through remotely sensed snow cover data or by using
169 the normalized difference vegetation index (NDVI) (Yannic *et al.*, 2014). One such remotely

170 sensed source of data of which the spatiotemporal resolution, extent and accuracy is rapidly
171 improving is satellite-based land-surface temperatures (LST) (Wan, 2008; Wan *et al.*, 2015).
172 Remotely-sensed LST are now freely available at the global scale at the vegetation canopy or
173 land surface level, with a temporal resolution of days over a period of decades and with a
174 spatial resolution ranging from 30'' (ca. 1000 × 1000 m at the equator) to as fine as 1'' (ca. 30
175 x 30 m) (Cook, 2014). This type of data does have the advantage over free-air temperature
176 datasets like WorldClim or CHELSA of being a direct and contiguous measurement in space
177 and time, as opposed to data interpolation and temporal averaging from a network of weather
178 stations, yet might be strongly affected by land surface characteristics and cloud cover in the
179 area (Zellweger *et al.*, 2019). Thanks to the increasing availability of these long-term and
180 accurate time series, such satellite-based LST-datasets offer very promising research avenues
181 to fill the gap between local temperature measurements and global-scale climatic datasets.

182 These different approaches to obtain suitable climate data have been extensively explored
183 and applied in SDMs (Bramer *et al.*, 2018), yet a comparative study of all of these
184 (downscaled and interpolated macroclimate data, field measurements, and satellite-based
185 LST) together – both concerning their inherent characteristics and their role in SDMs - has up
186 till now been missing. Such a comparison is nevertheless urgently needed in order to quantify
187 the progress that can be made by replacing the traditional global climate models with other
188 temperature data sources. We hypothesize in that regard that the best result depends in large
189 on two critical factors: a) the climatic characteristics of the study region, and b), the growth
190 forms of the study organisms. Here, we use a case study along steep climatic gradients in the
191 Northern Scandes, a mountain range in northern Scandinavia, to assess both factors and to
192 provide guidelines for the use of temperature data in SDMs in topographically challenging
193 regions. We compare the characteristics of different temperature datasets within the region, as
194 well as the descriptive and predictive power of SDMs for 50 plant species with different

195 growth forms: forbs, graminoids, (dwarf) shrubs and trees. We compare global climate
196 datasets (i.e. WorldClim and CHELSA) with datasets of remotely-sensed LST (MODIS), a
197 topographic downscaling and interpolation approach, and soil temperature obtained with
198 miniature data loggers, and use three widely applied and ecologically relevant (i.e.
199 bioclimatic) temperature variables: (i) mean annual temperature and mean temperature of the
200 (ii) warmest and (iii) coldest quarter. We hypothesize a significant effect of the spatial
201 resolution of the climate data, as well as of measurement focus (free-air, surface, or soil) and
202 temporal extent on temperature patterns across topographic gradients. Increasing
203 spatiotemporal accuracy of temperature data, especially through the use of *in-situ*
204 measurements, is expected to improve the descriptive and predictive power of the SDMs,
205 despite the associated loss in temporal extent. The optimal resolution, extent and
206 measurement focus are, however, likely to depend on the growth forms of the assessed
207 species, i.e. the spatiotemporal framework in which they operate.

208 **Methods**

209 *Study region*

210 The study was conducted in the Northern Scandes mountain range in Norway and Sweden,
211 between N 67°46'23.5" / E 16°30'52.6" (south west) and N 68°40'33.6" / E 18°58'40.4"
212 (north east), covering an area of 100 × 100 km and an elevation range from 0 up to 2097 m
213 a.s.l. The area ranges from the Norwegian coast, with a relatively mild and wet climate
214 dominated by birch forests with heathland understory, to the significantly drier and colder
215 eastern side of the Northern Scandes, typically vegetated by subarctic, alpine dwarf shrub
216 vegetation (Lembrechts *et al.*, 2014). The region was chosen for its strong climatic gradient,
217 with large macro- and microclimatic variation due to a distinct topography and high latitude

218 location (Scherrer & Körner, 2011; Graae *et al.*, 2012; Lenoir *et al.*, 2013). In total, 106
219 temperature measurement locations were spread across the study area (Fig. 1).

220 *Climate data*

221 For this area, we obtained eight different types of climate data encompassing a wide range of
222 measurement foci, spatiotemporal resolutions and temporal extents (Table 1). For each of
223 these datasets, we extracted or calculated the mean annual temperature and mean temperature
224 of the warmest and coldest quarter (bioclimatic variables Bio1, Bio10 and Bio11, following
225 the definition of WorldClim, Hijmans *et al.*, 2005, hereafter called mean annual, summer and
226 winter temperature, respectively). These ecologically relevant variables belong to the set of
227 physiologically most pertinent bioclimatic determinants of spatial plant species distribution
228 and are thus commonly used in SDMs (e.g. Austin & Van Niel, 2011; Cord & Rödder, 2011;
229 Distler *et al.*, 2015), and they allow us to accurately take into account seasonal differences in
230 climate. The different datasets are discussed in detail below.

231 a) WorldClim

232 The WorldClim database (Version 2.0) provides globally interpolated free-air temperature
233 conditions over a 30-year time period (1970-2000) at a spatial resolution of 30'' (ca. 1000 ×
234 1000 m at the equator) (Fick & Hijmans, 2017). The studied bioclimatic variables were
235 directly downloaded from the website (www.worldclim.org).

236 b) CHELSA

237 The climatologies at high resolution for the earth's land surface areas (CHELSA, Version 1.2)
238 is a global dataset based on quasi-mechanistical statistical downscaling of free-air
239 temperatures from the ERA Interim (ECMWF) global circulation model (Dee *et al.*, 2011),
240 over a period of 34 years (1979-2013) and with the same spatial resolution as WorldClim

241 (30'', ca. 1000 x 1000 m at the equator), yet for a more recent time period (Karger *et al.*,
242 2017). Bioclimatic variables were again downloaded directly from the website (www.chelsa-
243 climate.org).

244 c) Downscaled CHELSA-data (hereafter called 'downscaled')

245 We used the bioclimatic variables downloaded from CHELSA, at an original resolution of
246 30'' (ca. 1000 x 1000 m at the equator), and downscaled them statistically even further, to a
247 1'' (ca. 30 × 30 m at the equator) resolution based on topographic variation, using a
248 physiographically-informed model fitted with a geographically weighted regression (GWR)
249 technique (Fotheringham *et al.*, 2003). In short, GWR extends the traditional regression
250 approach by allowing estimated regression parameters to vary across space. Therefore, GWR
251 models are particularly relevant to explore the scale-dependent and spatial non-stationary
252 relationships between free-air temperatures and physiographic variables (here: elevation,
253 slope, eastness, northness, distance to the ocean and clear-sky solar radiation) (Su *et al.*,
254 2012). For more details, see Supplementary Material 1.

255 d) Topoclimate

256 Fine-resolution gridded climate data for the region was obtained from Aalto *et al.* (2017), who
257 included topography-driven small-scale climate heterogeneity in a topoclimatic interpolation
258 of weather station data across northern Scandinavia, using generalized additive modelling at a
259 resolution of 1'' (ca. 30 x 30 m at the equator). They modelled monthly average temperatures
260 from 1981 till 2010 using geographical location, elevation, water cover, solar radiation and
261 cold-air pooling. Bioclimatic variables were calculated based on these monthly averages.

262 e) MODIS LST

263 The moderate resolution imaging spectroradiometer (MODIS) satellite TERRA (Wan *et al.*,
264 2015) from the National Aeronautics and Space Administration (USA) provides global land
265 surface temperature (LST). We extracted data from MOD11A2: 8-day averages based on the
266 clear sky day- and night-time records at a 30'' (ca. 1000 × 1000 m at the equator) resolution,
267 for a period of two years corresponding to the *in-situ* measurements (from August 2015 to
268 July 2017, see below). Mean annual temperature was calculated in ArcGIS by averaging the
269 temperature per pixel for 2015-2016 and 2016-2017, separately, from day of the year (DOY)
270 209 in year *n* (e.g. July 27th for 2015) till DOY 208 in year *n*+1 (e.g. July 26th for 2016),
271 which was the set of 8-day averages corresponding most closely with the period used for the
272 *in-situ* temperature measurements described below (see sub-section *h* on Soil temperatures).
273 Mean summer and winter temperatures were calculated similarly, yet for DOY 185 (e.g. July
274 3th in 2015) till 272 (September 28th in 2015) and from DOY 1 (e.g. January 1st in 2016) till
275 88 (March 28th in 2016), respectively.

276 f) EuroLST

277 The EuroLST dataset is a gap-filled dataset at the European scale of LST derived from
278 MODIS (see sub-section *e* focusing on MODIS LST) at a spatial resolution of 250 × 250 m
279 and averaged over a temporal extent of 10 years (Metz *et al.*, 2014). This dataset has been
280 created using a combination of weighted temporal averaging with statistical modelling and
281 spatial interpolation to fill in the gaps in the MODIS LST dataset, as well as to improve its
282 spatial resolution. Relevant bioclimatic variables were downloaded directly from the website
283 ([courses.neteler.org/eurolst-seamless-gap-free-daily-european-maps-land-surface-](https://courses.neteler.org/eurolst-seamless-gap-free-daily-european-maps-land-surface-temperatures)
284 [temperatures](https://courses.neteler.org/eurolst-seamless-gap-free-daily-european-maps-land-surface-temperatures)).

285 g) E-OBS

286 The E-OBS dataset (version 17.0) provides daily gridded climate data of free-air temperature
287 for Europe at a 0.1° (ca. 10.000×10.000 m at the equator) spatial resolution, interpolated
288 from weather stations (Haylock *et al.*, 2008), used here over the study period from August
289 2015 to July 2017 (as in sub-section *e* on MODIS LST). The gridded dataset is created by first
290 interpolating the monthly mean temperature from the weather stations using three-
291 dimensional thin-plate splines, interpolating the daily anomalies using a spatial kriging
292 approach with an external drift for temperature, and then combining these monthly and daily
293 estimates. Temperature data was downloaded directly from the website
294 (<https://www.ecad.eu/download/ensembles/download.php>) and subsequently used to generate
295 the three studied bioclimatic variables in R.

296 h) Soil temperatures

297 Near-surface soil temperatures were logged every 1.5 or 2 hours (iButtons: DS1922L or
298 DS1921G, with 0.5°C accuracy, www.maximintegrated.com, San José, CA, USA) at a depth
299 of 3 cm below the soil surface in 106 locations along several elevation gradients in Norway
300 and Sweden (Fig. 1, Table 2). Loggers were wrapped in parafilm and put in a small zipper bag
301 to prevent water damage. The loggers were originally established for several different projects
302 (Lembrechts *et al.*, 2014; Lembrechts *et al.*, 2016; Lembrechts *et al.*, 2017) along seven
303 elevation gradients, together ranging from 0 to 1200 m a.s.l., of which three were in Norway
304 and four in Sweden. The three bioclimatic variables were calculated in R (R Core Team,
305 2015) for each 106 locations and for each year (from 2015 till 2017, corresponding to the
306 periods used in sub-section *e*) from daily averages. Based on these soil temperature data, we
307 made predictions for each bioclimatic variable for the whole study area of 100×100 km for
308 the period August 2016 till July 2017 using GWRs (as in sub-section *c* featuring the
309 downscaling approach) based on the same physiographic variables (i.e. elevation, slope,
310 eastness, northness, distance to the ocean and clear-sky solar radiation). The models were

311 used to predict the bioclimatic variables for every 1'' (ca. 30 x 30 m at the equator) pixel in
312 the study area. For more details on the interpolation approach, see Supplementary Material 1.

313 ***Plant species observations***

314 Plant species data were obtained during summer 2017 in the framework of the Mountain
315 Invasion Research Network (www.mountaininvasions.org) long-term monitoring effort, and
316 specifically as a follow-up of the survey of Lembrechts *et al.* (2014) in the Norwegian study
317 plots (59 out of the 106 plots with *in-situ* soil temperature measurements, see Fig. 1, Table 2).
318 Within the framework of this survey, three elevation gradients were selected (spanning on
319 average 700 m in elevation). The elevation range covered by each gradient was divided into
320 19 equally spaced elevation bands, resulting in 20 sampling sites per gradient. At each
321 elevation, presence/absence of all vascular plant species was recorded in plots of 2 × 50 m in
322 natural vegetation. At one end of each of these plots, the temperature logger (see dataset
323 described in sub-section *h* above) was buried. We used data for the 50 most common plant
324 species in the survey (i.e. at least 10 occurrences). Species were grouped based on their
325 growth forms (Table S1): forbs (N = 25); graminoids (N = 7); dwarf shrubs (N = 15); and
326 trees (N = 3). All species were native to the region.

327 ***Direct comparison of climatic variables***

328 1) Relation to elevation

329 To assess differences in the behaviour of the eight climate datasets along an elevation
330 gradient, the three bioclimatic variables derived from these climate datasets were plotted
331 separately against the elevation of the 106 locations of the *in-situ* soil temperature data
332 loggers. For the gridded climate datasets, we extracted a value for each bioclimatic variable
333 for each location. We used linear models (function *lm* in R, R Core Team, 2015) to assess the
334 lapse rate (i.e. the slope, °C per 100 m) of temperature decrease with elevation. For MODIS

335 LST, E-OBS and the soil temperature measurements, data was plotted and modelled
336 separately for the two study years (2015-2016 and 2016-2017).

337 2) Paired comparisons

338 For each of the 106 studied locations, we compared the values for each climatic dataset (and
339 each of the three bioclimatic variables) against the others, to investigate consistent
340 temperature deviations between datasets. Trends for each bioclimatic variable and each
341 dataset were visualised with general additive models (GAMs) with a cubic regression line and
342 without pre-set smoothing value (function `gam`, R package `mgcv`, Wood, 2006), following
343 procedures described in Zuur *et al.* (2009). GAMs were used as we did not want to make
344 restrictive assumptions about the relationships of the datasets with each other.

345 3) Correlative dendrograms

346 For all 106 locations, we made correlative dendrograms (distance = $1 - \rho$, where ρ is the
347 Pearson's product-moment correlation) to visualize correlations among and relationships
348 between the different datasets, using the function `hclust` from the package `spatstat` (Baddeley
349 *et al.*, 2015).

350 4) Regional climate predictions

351 We generated regional maps for the different climate datasets (see the Climate data section as
352 well as Supplementary Material 1 for more details on how the maps were generated for the in-
353 situ measurements), and calculated for each pixel the absolute temperature difference between
354 the respective dataset and the regionally modelled soil temperature at a 1'' (ca. 30 × 30 m at
355 the equator) spatial resolution.

356 5) Temporal correction

357 For a more formal comparison between the datasets with different temporal windows, we
358 calculated for each climatic dataset its difference with the ‘background climate’, taken as
359 temperatures for the window in question from the ERA Interim (ECMWF) 2 meter free-air
360 temperature database (Dee *et al.*, 2011). This is a time series of monthly means of daily means
361 from 1979 up till 2018 (hence covering the time period for all studied datasets except
362 WorldClim), for which we calculated average Bio1, Bio10 and Bio11 over the whole $100 \times$
363 100 km study area (based on the original $0.75^\circ \times 0.75^\circ$ resolution grid). We then re-ran the
364 paired comparisons (see above) with the temperature off-set, i.e. the difference between the
365 bioclimatic value (for each observation and for each dataset) and the average bioclimatic
366 value from ERA Interim for the corresponding period, using paired t-tests to test for potential
367 differences, e.g. differences between a) $\text{Bio1}(\text{soil temperature}_{(2016-2017)}) - \text{Bio1}(\text{ERA}$
368 $\text{Interim}_{(2016-2017)})$ and b) $\text{Bio1}(\text{CHELSA}_{(1979-2013)}) - \text{Bio1}(\text{ERA Interim}_{(1979-2013)})$.

369 Using this off-set of temperatures from a standardized and common time series allowed to
370 correct to some extent for differences in the temporal scope among the climatic datasets, and
371 thus climate change and inter-annual weather variation. While this does not take into account
372 possible decoupling of climate change between soil, surface and air temperature, it does allow
373 to estimate the size of the temporal effect in the dataset, and thus quantify the difference
374 between in-situ soil temperature and the other datasets more precisely.

375 ***Species distribution modelling***

376 The regional distribution of the 50 plant species was modelled using species-specific
377 generalized linear mixed-effect models (GLMMs) (function *glmer*, package *lme4* (Bates *et*
378 *al.*, 2013), family = binomial) as a function of mean annual, summer and winter temperature,
379 and their quadratic terms. Gradient (plant data were available from three different elevation
380 gradients; Table 2) was used as a random intercept term in these models to account for

381 structural variation between gradients. This was repeated for each climate dataset (except for
382 E-OBS, as due to the limited measured climate variation within the region, species
383 distributions could not be modelled), resulting in a total of 350 SDMs (50 species \times 7
384 datasets). For both MODIS LST and soil temperature, only the data from the measurement
385 year prior to the species observations (2016-2017) were used, while the bioclimatic variables
386 from 2015-2016 were highly correlated with those of 2016-2017 and thus excluded. The
387 variance inflation factor (VIF, function `vif`, package `car`, Fox & Weisberg, 2011) was
388 calculated for each of the climatic datasets to test the correlation between the different
389 bioclimatic variables. As the VIF (a value between 0 and infinity) exceeded 5 (indicating a
390 strong correlation) for some datasets (specifically those with long-term climatic averages),
391 separate models including only Bio1 as explanatory variables were made, and results
392 compared between both approaches.

393 The explained variance in the present distribution of the species (R^2 of the fixed effect, i.e. the
394 marginal R^2 , Nakagawa & Schielzeth, 2013) was then calculated for each model and
395 compared across all species between the different datasets with an ANOVA and a post-hoc
396 Tukey HSD test ($R^2 \sim$ growth forms (factor with 4 levels), model assumptions were met). We
397 also compared the increase in R^2 values obtained by using soil temperature versus the other
398 climate datasets for the different growth forms (forbs, graminoids, shrubs and trees)
399 separately.

400 Finally, we assessed the predictive power of the different SDMs using a leave-one-out
401 method, each time calibrating the model with 59 data points (plots) and predicting for the
402 remaining one. We calculated the area under the curve (AUC) of the receiver operation
403 characteristic (ROC), using the function `performance` from the package `ROCR` (Sing *et al.*,
404 2005), as well as the sensitivity (presences correctly predicted as presences) and the
405 specificity (absences correctly predicted as absences) metrics. A value of 0.5 was used to

406 binarize predictions. This was repeated for each species and for each climate dataset, and
407 differences in AUC, sensitivity and specificity between SDMs using the different climatic
408 datasets were again assessed with an ANOVA and a post-hoc Tukey HSD test. We also
409 compared the increase in AUC, sensitivity and specificity obtained by using soil temperature
410 versus the other climate datasets for the different growth forms separately. Note that this
411 predictive approach is limited for three reasons: First, the restricted dataset size likely
412 constrains the predictive power of the models. Secondly, for comparison purposes, our SDMs
413 are only calibrated using bioclimatic predictors, and thus predictive power (as estimated here
414 using AUC-values) will be relatively low. Thirdly, when using predictive modelling in small-
415 sized plots (i.e. 100 m² here, vs. 1 km² traditionally), one can expect a high accuracy in
416 correctly predicting presences as presence (i.e. if a species is observed, the model will also
417 predict its presence), yet low accuracy in predicting absences as absence (i.e. if a species is
418 absent, this could either be due to the plot falling outside its niche (correctly predicted
419 absence), or due to random absences due to the limited plot size, or microscale non-climatic
420 factors (incorrectly predicted absence)). Of course, incorrect absences can also be due to
421 observation bias, identification uncertainties and incomplete detection, further lowering
422 predictive power. We thus expect high sensitivity, yet relatively low specificity and AUC-
423 values, and encourage interpretation of these different evaluation metrics together to assess
424 the predictive power of the models (Jiménez-Valverde, 2012).

425 All analyses were performed in R (R Core Team, 2015).

426 **Results**

427 *Direct comparison of climatic variables*

428 All three studied bioclimatic variables (Bio1 = mean annual, Bio10 = mean summer and
429 Bio11 = mean winter temperature) showed a consistent negative correlation with elevation in

430 almost all temperature datasets in the region, yet with large differences in lapse rate (Fig. 2).
431 The latter ranged for mean annual temperature from around $-0.6\text{ }^{\circ}\text{C}$ per 100 m for CHELSA,
432 downscaled CHELSA and Topoclimate, over around $-0.4\text{ }^{\circ}\text{C}$ per 100 m for WorldClim,
433 EuroLST and MODIS LST to $-0.2\text{ }^{\circ}\text{C}$ per 100 m for soil temperature and $-0.1\text{ }^{\circ}\text{C}$ per 100 m
434 for E-OBS. Mean annual temperatures were in both years consistently higher for the soil
435 temperature than for all other datasets, i.e. both the long-term temperature data (WorldClim,
436 CHELSA, downscaled CHELSA, Topoclimate and EuroLST, Fig. 3a-e) and the surface
437 (MODIS LST, Fig. 3f) and free-air (E-OBS, Fig. 3g) temperature measurements from the
438 same time period ($p < 0.001$ from a linear model), yet differences were larger at low than at
439 high temperatures. Differences of 3 to 6 $^{\circ}\text{C}$ between soil temperature and all other datasets
440 remained even after correcting for possible inter-annual and climate change effects (Table 3,
441 Fig. S1a-f). Significant differences of up to 3 $^{\circ}\text{C}$ in mean annual temperature could also be
442 observed between all other datasets (Table 4, Fig. S2).

443 Despite the higher mean annual temperature in the soil, mean summer soil temperature was in
444 both years similar (compared to WorldClim, Topoclimate, EuroLST and E-OBS) or even
445 lower (CHELSA, downscaled CHELSA and MODIS LST) than air and surface temperature
446 (Fig. 3h-n). After correcting for inter-annual and climate change effects, differences between
447 soil temperature and most other datasets (except MODIS LST) remained limited to around 1
448 to 1.5 $^{\circ}\text{C}$ (Table 4, Fig. S1g-l). Summer temperature recordings were highest in MODIS LST
449 (Fig. 2n, Fig. S2i,k,l). The relationship with elevation was again the strongest for
450 (downscaled) CHELSA ($-0.6\text{ }^{\circ}\text{C}$ per 100 m), and weakest for E-OBS and MODIS LST.

451 Winter temperature showed the largest discrepancy between soil, free-air and surface
452 temperatures (Fig. 3), with soil temperatures being close to 0 $^{\circ}\text{C}$ from sea level up to at least
453 900 m a.s.l., and as such driving the higher mean annual temperatures in the soil (Fig. 2x).
454 Part of this variation was due having relatively warm winters with plenty of snow in the area

455 in the period 2015-2017, yet the difference remained as high as 4 °C to 11 °C after correcting
456 for the temporal mismatch (Table 4, Fig. S1n-r). Surface temperatures were in addition colder
457 than free-air temperatures (Fig. S2n-r) due to an extended frost period (Fig. S3). Temperature
458 differences between years were relatively small, except for mean annual and mean summer
459 surface temperatures from MODIS (Fig. 2f,n).

460 The above-mentioned differences along the elevation gradient, combined with additional
461 effects from local topography, resulted in large regional differences between the different
462 climate datasets in general (Fig. 4), and between interpolated soil temperature and the other
463 datasets in particular (Fig. 5). The correlation analyses (Fig. 4) showed that the climate
464 datasets were nested, with strongest relationships (across all bioclimatic variables) between
465 the datasets with long-term averages: (downscaled) CHELSA, Topoclimate, WorldClim and
466 EuroLST. The datasets with short-term measurements (in-situ soil, MODIS LST and free-air
467 E-OBS) differed more from each other than from the long-term averages. Modelled mean
468 annual temperature in the soil was, as expected, several degrees warmer than in all other
469 datasets, especially at higher elevations (Fig. 5), while in summer soil temperature was
470 warmer than CHELSA climate and MODIS LST at high elevations, yet colder at low
471 elevations (Fig. 5). Winter temperature predictions were up to 17 °C higher in the soil than in
472 the other datasets, except at the highest elevations. Due to the large local variation in snow
473 cover, however, winter soil temperature predictions were unreliable (Fig. 5, Fig. S3), in
474 contrast to annual and summer temperatures, for which the local R^2 (indicating the local
475 spatial regression fit) of the regional interpolations was highly consistent across space, albeit
476 only moderately high, i.e. on average 50% for Bio10 and 37% for Bio1.

477 *Species distribution modelling*

478 SDMs using soil temperatures explained on average 80% of variance (48% if only Bio1 was
479 used), which was on average 18% (15% for models with Bio1 only) more than the models
480 using other climate datasets (Fig. 6, significant differences with most datasets after correcting
481 for multiple testing). Differences in explained variance among SDMs based on these other
482 datasets were much smaller. Differences in predictive power were not significant between
483 models (highest for Euro-LST and downscaled CHELSA (AUC \approx 0.70), and between 0.61
484 and 0.64 for the other datasets (Fig. S5). As expected, sensitivity was high (\approx 0.85), yet
485 specificity was low (\approx 0.27) for all datasets. Predictive modelling was nearly impossible with
486 models with Bio1 only (AUC \approx 0.5, specificity \approx 0.20), even though sensitivity was still high
487 (\approx 0.81).

488 Model performances depended strongly on growth forms (i.e. forbs, graminoids, dwarf
489 shrubs, trees, Fig. 6b-c). We observed a significant net improvement in marginal R^2 values (as
490 an indicator of descriptive power of the models) for SDMs based on soil temperature in the
491 case of forbs and graminoids compared to the other datasets (on average +24% and +21% for
492 the full model, respectively, and 20% and 25% for the model with Bio1 only), and moderately
493 so for shrubs (full model: +8%, Bio1: +25%). Yet there was no such net increase for trees
494 (+2% and 8% only). On the contrary, we observed a significant net decrease in predictive
495 values for shrubs and trees when using soil temperature compared to most of the other
496 datasets (AUC on average -0.12 and -0.11 respectively for both models; -0.06 and -0.08 for
497 Se), yet not so for forbs and graminoids (Fig. S5b-c).

498 **Discussion**

499 Our comparison of different climate datasets highlights that the use of a specific source of
500 climate data is species- and region-specific and can have strong repercussions on the outcome
501 of SDMs, as exemplified here for the distributions of 50 plant species along steep climatic

502 gradients in a cold-climate region. Our data indeed revealed a strong sensitivity of SDMs to
503 the used climate dataset depending on the growth form of the species. In general, the use of
504 *in-situ* soil temperature instead of surface or free-air temperature did improve the explanatory
505 power of our SDMs. It did so much more for forbs and graminoids, to a lesser degree for
506 shrubs, yet not for trees (Fig. 6). This outcome confirms recent studies arguing for the use of
507 more local climate variables in distribution modelling (e.g. Ashcroft *et al.*, 2008; Pradervand
508 *et al.*, 2014; Slavich *et al.*, 2014; Opedal *et al.*, 2015; Meineri & Hylander, 2017) and proofs
509 the validity of this concept across a whole range of possible temperature data sources. Yet,
510 our results also indicate that an increased accuracy of climate data does not necessarily
511 improve distribution models for all species or in all circumstances (Bennie *et al.*, 2014;
512 Pradervand *et al.*, 2014), as it will depend on the growth forms of the species and perhaps also
513 the regional climate characteristics. The differences in SDMs' explanatory power could result
514 from differences in measurement focus and spatiotemporal resolution or extent, related to the
515 different spatiotemporal framework in which different species groups operate, as discussed
516 below.

517 ***Measurement focus***

518 The most critical differences observed between the climate datasets in this study were likely
519 driven by measurement focus (free-air, land surface or soil), with consistently higher average
520 annual temperatures observed in the soil resulting to a large extent from differences in winter
521 temperatures (Bio11). Even though free-air temperature predictions (WorldClim, CHELSA,
522 E-OBS) for winter temperature easily dropped below $-7\text{ }^{\circ}\text{C}$, and surface temperature
523 measurements (EuroLST, MODIS LST) were even lower, winter temperatures just below the
524 soil surface were close to $0\text{ }^{\circ}\text{C}$ along most of the elevation gradient (Fig. 2). Only in those
525 locations where global climate models predicted an average winter temperature below $-10\text{ }^{\circ}\text{C}$,
526 measured soil temperatures dropped below $0\text{ }^{\circ}\text{C}$ (Fig. 2). These differences remained even

527 after correcting for the temporal mismatch in the different datasets (Table 4, Fig. S1). While
528 some of the earliest studies on soil temperature reported a strong relationship with air
529 temperature across all seasons (Shanks, 1956), it is clear that both a dense vegetation cover
530 and a thick snowpack can provide effective insulation and protection against freezing events
531 in the subnivium (Geiger, 1950; Dorrepaal *et al.*, 2004; Pauli *et al.*, 2013; Aalto *et al.*, 2017;
532 Thompson *et al.*, 2018), and that snow in the Arctic is a crucial explanatory variable for the
533 distribution of plant species (Randin *et al.*, 2009a; Niittynen & Luoto, 2017). In northern
534 Norway, especially, the relatively mild climate and humid air from the ocean result in thick
535 winter snow packs that can provide a significant decoupling between air, surface and soil
536 temperature (Pauli *et al.*, 2013; Thompson *et al.*, 2018). Such an insulating snow pack can
537 affect plant life in several ways, through its effects on overwintering survival, productivity,
538 reproductive success and nutrient and water availability (Niittynen & Luoto, 2017), with both
539 positive (e.g. less frost events) and negative effects (e.g. limited growing season) observed.
540 For many species in the region, especially low-growing forbs and graminoids, we have shown
541 that using near-surface soil temperatures instead of free-air temperatures, which allows
542 incorporating these snow cover effects, is crucial to accurately describe the distribution of
543 small-stature plants (Randin *et al.*, 2009a; Niittynen & Luoto, 2017). For trees, however, the
544 absence of model improvement through the use of soil temperature might result from a
545 stronger correlation with air than with soil temperature due to higher maximum canopy
546 heights, at least in later life stages. In winter and early spring, trees are likely to be much more
547 affected by air temperatures and freezing events affecting their buds above the snow than by
548 temperatures in the soil (Körner, 2003).

549 These results also indicate that the relative importance of using soil temperature in SDMs will
550 depend on the topography and large-scale climate of the region. Most importantly, the amount
551 of fresh snow in winter will define the strength of the discrepancy between winter (and thus

552 indirectly annual) mean temperatures in the soil and in the air (Cohen, 1994; Zhang, 2005).
553 The mismatch is in our study indeed significantly larger in the warmer but snowier
554 (Norwegian) plots at low elevations than in the colder yet drier (Swedish) plots at high
555 elevations (Fig. 3). For summer temperature, our data overall showed a more consistent
556 match between the different datasets, although with minor buffering effects of the vegetation.
557 Even though the discrepancy between measurement foci is thus region-specific (and likely
558 even more different in e.g. tropical regions), we suggest that the use of climate data in close
559 proximity to the study species is always recommended. Importantly, however, the use of soil
560 temperature does not fully resolve this measurement mismatch, as only part of the plants are
561 belowground. Although our data demonstrates a significant improvement in the use of soil
562 temperature over free-air temperature data for species groups entirely covered by snow in
563 winter, an optimal approach would incorporate in-situ climate measurements both above and
564 below the soil surface. The latter can for example be achieved with the temperature and soil
565 moisture plant simulator sensors as described in Wild *et al.* (2019), measuring temperatures
566 at, above and below the surface.

567 Despite the clear benefits of using soil temperature data in SDMs, a major drawback (next to
568 the cost associated with obtaining *in-situ* soil temperature measurements) lies in the increased
569 local-scale heterogeneity, especially in winter. The soil temperatures were in our study indeed
570 hard to predict accurately using a 50 × 50 m DEM-based interpolation approach. More *in-situ*
571 temperature measurements, as well as the inclusion of other microclimate-related variables
572 like snow cover maps, might be needed to improve interpolations of microclimate at fine
573 spatial resolution. This is also a prerequisite for better SDMs' predictive performances.
574 Follow-up studies with larger datasets and in-situ measurements of more environmental
575 variables (e.g. soil moisture, air temperature, precipitation, or snow cover) are thus
576 recommended to investigate this further.

577 While satellite-measured land surface temperature data (MODIS LST and EuroLST) resulted
578 in mean annual temperatures within the same range as those obtained with free-air
579 temperature measurements, the land surface temperatures were, throughout the measurement
580 period, significantly higher in summer and lower in winter, thus resulting in an increased
581 overall annual temperature range (Fig. 2, Fig. S1, Table 4). These extremes were however
582 smoothed out when using the EuroLST temperature averages over a ten-year period. While
583 the use of satellite-based land surface temperature for SDMs has until now been largely
584 underexplored, our study adds to the growing list of recent studies indicating the potential of
585 these untapped data resources for accurately predicting species distributions (see e.g. Cord &
586 Rödder, 2011; Bisrat *et al.*, 2012; Neteler *et al.*, 2013). We expect that LST-timeseries with an
587 even higher spatial resolution, such as Landsat (Cook, 2014) will as such turn out the crucial
588 link between local-scale temperature measurements and global climate models. Our results
589 however indicate that smoothed, long-term averages like EuroLST are preferable above short-
590 term measurements, especially for predictive modelling. Similar to the issue of spatial
591 heterogeneity for *in-situ* soil temperature data, averages over long-term time series are, by
592 nature, more likely to increase the predictive performances of SDMs compared with more
593 erratic fluctuations based on short-term data.

594 *Temporal - extent*

595 Differences between the used climate datasets could also be attributed to variation in temporal
596 extent, with the datasets building on long-term historic averages (WorldClim, CHELSA,
597 Topoclimate and EuroLST) showing the strongest correlation with each other (Fig. 4).
598 Correlations were however weakest for the three datasets with only two years of data, yet with
599 different measurement foci as described above (MODIS LST, E-OBS and soil temperature).
600 While patterns over time for these datasets were relatively consistent between measurement
601 years (Fig. 2), they did reveal more variation between air and surface temperature than

602 between EuroLST and the other datasets with long-term climatic averages. The discrepancy in
603 temporal extents might also explain why the performance of our predictive models decreased
604 in some cases for shrubs and trees when using short-term soil (or surface) temperatures (Fig.
605 S4 and 5). These long-lived species are indeed likely to be relatively inert towards short-term
606 changes in their environment (Körner, 2003), which might make it harder to predict their
607 distribution based on locally-measured short-term temperatures (Ashcroft *et al.*, 2008). Long-
608 lived organisms like most arctic-alpine species in the study region could also persist outside
609 their niche for considerable parts of their life (Bond & Midgley, 2001), adding to the
610 complexity of predicting their distribution using short-term temperature data.

611 ***Spatial resolution***

612 Our comparative approach indicates that the downscaling or interpolation of climate data – as
613 applied here respectively to global datasets like CHELSA and the *in-situ* soil temperature
614 data and topoclimatic dataset from Aalto *et al.* (2017) – was rather successful. Downscaling
615 of CHELSA from 1000×1000 m to 30×30 m based on the physiography worked well, as
616 indicated by the high local R^2 -values (0.90 ± 0.06 for Bio1 and Bio10, 0.89 ± 0.06 for Bio11,
617 Fig. S4), yet nevertheless only resulted in minor improvements of the regional SDMs
618 compared to coarse-grained CHELSA-data (3.7% and 0.035 for the R^2 and AUC values,
619 respectively). This lack of improvement is in disagreement with several other studies (e.g.
620 Gillingham *et al.*, 2012; Slavich *et al.*, 2014). Part of this could be due to the inherent
621 limitations in the original CHELSA dataset: unlike elevation, small-scale topographic
622 variables like slope and aspect are not taken into account into the original CHELSA model,
623 and their inclusion in the downscaling approach is thus unlikely to have major effects. Small-
624 scale topographic effects on microclimate are more correctly taken into account in the
625 topoclimatic dataset from Aalto *et al.* (2017), however, making the latter approach
626 recommendable above the former. The fact that the topoclimatic dataset did not perform

627 significantly better in the SDMs than CHELSA either ($\Delta R^2 = -7\%$ and $+5\%$, and $AUC = -0.01$
628 and $+0.06$, depending on the model), might suggest again that an increased level of detail is
629 not better by default, yet depends on the context of the study (Bennie *et al.*, 2014). The most
630 likely explanation for this lack of improvement in model performance in this case thus is that
631 the distribution of the studied alpine species might be less driven by small-scale topoclimatic
632 variation in air temperature than by snow-cover induced variation in soil temperature.

633 Interpolation of the soil temperature data worked well across the whole study region, except
634 for winter temperature, where probably the strong local variation and the highly non-linear
635 correlation with elevation resulted in inaccurate predictions (Figure 4, Fig. S3, Ashcroft *et al.*,
636 2008). The large differences in winter temperatures between measurement locations – and the
637 low predictability of soil winter temperature in the region – thus suggest that caution is
638 needed, as in many regions winter temperatures are likely crucial for the distribution of
639 species (Williams *et al.*, 2015). A larger dataset and more accurate predictor variables, e.g.
640 related to snow cover duration (Niittynen & Luoto, 2017), might be needed to improve these
641 interpolation efforts.

642 ***Implications***

643 The observed differences in the climate datasets and SDMs at the regional scale advocate for
644 a careful selection of the climate data source when modelling species distributions, based on a
645 priori ecological assumptions about the relationship of the studied organism with the regional
646 environment, and the comparison – or joint use – of different datasets (Buermann *et al.*, 2008;
647 Rebaudo *et al.*, 2016). Measurement focus, temporal extent and spatiotemporal resolution
648 should all be taken into account with regard to the studied species and area: is the species
649 affected by snow cover; is it an annual or a perennial species; is the focal species mobile or
650 sessile; does the study area reach above the treeline; is it in topographically challenging

651 terrain, etc. Our study highlights the importance of growth forms: soil temperature was highly
652 important for forbs and graminoids, and to a certain extent for shrubs, yet not so for trees.
653 Only when making ecologically meaningful a priori decisions, and when comparing the
654 performance of different datasets – and perhaps their interactions, one can be sure that the
655 observed trends relate to the actual (micro)climate experienced by the study species or species
656 group(s) in the study region. Understanding these processes in the current climate is a crucial
657 step before model projections can be improved under climate change as well. In order to
658 advance towards this goal, there is an urgent need for large-scale datasets of microclimate
659 data; ecologists and climatologists should consider in-depth on-the-ground, long-term
660 microclimate monitoring along climatic gradients to be able to improve our microclimatic
661 models for use in SDMs (Lembrechts *et al.*, 2018). Nevertheless, our case study suggests that
662 SDMs can be relatively robust to several characteristics of different types of climate datasets,
663 like spatial and temporal resolution, especially in the relatively stable slow-reacting
664 vegetation types of high-latitude mountains. Additionally, there is a need to improve our
665 abilities to forecast microclimate data itself in the future, as climate change is likely to affect
666 soil, surface and air temperatures differently (Ashcroft & Gollan, 2013; De Frenne *et al.*,
667 2019). Significant progress has been made in this regard, for example by integrating
668 microclimatic dynamics and processes like microclimatic buffering in predictions (Keppel *et*
669 *al.*, 2015; Lenoir *et al.*, 2017; Wason *et al.*, 2017), yet there is still a need for improvement
670 before the same diversity and quality of climate datasets will be available for SDM
671 projections into future climate as we have now for current climate.

672 **References**

673 Aalto, J., Riihimäki, H., Meineri, E., Hylander, K. & Luoto, M. (2017) Revealing topoclimatic
674 heterogeneity using meteorological station data. *International Journal of Climatology*, **37**,
675 544-556.

676 Aalto, J., Scherrer, D., Lenoir, J., Guisan, A. & Luoto, M. (2018) Biogeophysical controls on soil-
677 atmosphere thermal differences: implications on warming Arctic ecosystems. *Environmental*
678 *Research Letters*, **13**, 074003.

679 Ashcroft, M.B. (2010) Identifying refugia from climate change. *Journal of Biogeography*, **37**, 1407-
680 1413.

681 Ashcroft, M.B. & Gollan, J.R. (2012) Fine-resolution (25 m) topoclimatic grids of near-surface (5 cm)
682 extreme temperatures and humidities across various habitats in a large (200 x 300 km) and
683 diverse region. *International Journal of Climatology*, **32**, 2134-2148.

684 Ashcroft, M.B. & Gollan, J.R. (2013) Moisture, thermal inertia, and the spatial distributions of near-
685 surface soil and air temperatures: Understanding factors that promote microrefugia.
686 *Agricultural and Forest Meteorology*, **176**, 77-89.

687 Ashcroft, M.B., Chisholm, L.A. & French, K.O. (2008) The effect of exposure on landscape scale soil
688 surface temperatures and species distribution models. *Landscape Ecology*, **23**, 211-225.

689 Austin, M.P. & Van Niel, K.P. (2011) Improving species distribution models for climate change studies:
690 variable selection and scale. *Journal of Biogeography*, **38**, 1-8.

691 Baddeley, A., Rubak, E. & Turner, R. (2015) *Spatial Point Patterns: Methodology and Applications with*
692 *R*.

693 Bates, D., Maechler, M., Bolker, B. & Walker, S. (2013) lme4: linear mixed-effects models using Eigen
694 and S4. In, R package version 1.0-5.

695 Bennie, J., Wilson, R.J., Maclean, I.M.D. & Suggitt, A.J. (2014) Seeing the woods for the trees - when is
696 microclimate important in species distribution models? *Global Change Biology*, **20**, 2699-
697 2700.

698 Bisrat, S.A., White, M.A., Beard, K.H. & Richard Cutler, D. (2012) Predicting the distribution potential
699 of an invasive frog using remotely sensed data in Hawaii. *Diversity and Distributions*, **18**, 648-
700 660.

701 Bond, W.J. & Midgley, J.J. (2001) Ecology of sprouting in woody plants: the persistence niche. *Trends*
702 *in ecology & evolution*, **16**, 45-51.

703 Bramer, I., Anderson, B., Bennie, J., Bladon, A., De Frenne, P., Hemming, D., Hill, R.A., Kearney, M.R.,
704 Körner, C., Korstjens, A.H., Lenoir, J., Maclean, I.M.D., Marsh, C.D., Morecroft, M.D.,
705 Ohlemüller, R., Slater, H.D., Suggitt, A.J., Zellweger, F. & Gillingham, P.K. (2018) Advances in
706 monitoring and modelling climate at ecologically relevant scales. *Advances in Ecological*
707 *Research*,

708 Buermann, W., Saatchi, S., Smith, T.B., Zutta, B.R., Chaves, J.A., Milá, B. & Graham, C.H. (2008)
709 Predicting species distributions across the Amazonian and Andean regions using remote
710 sensing data. *Journal of Biogeography*, **35**, 1160-1176.

711 Cohen, J. (1994) Snow cover and climate. *Weather*, **49**, 150-156.

712 Cook, M.J. (2014) Atmospheric Compensation for a Landsat Land Surface Temperature Product.

713 Cord, A. & Rödder, D. (2011) Inclusion of habitat availability in species distribution models through
714 multi-temporal remote-sensing data? *Ecological Applications*, **21**, 3285-3298.

715 De Frenne, P., Zellweger, F., Rodríguez-Sánchez, F., Scheffers, B.R., Hylander, K., Luoto, M., Vellend,
716 M., Verheyen, K. & Lenoir, J. (2019) Global buffering of temperatures under forest canopies.
717 *Nature Ecology & Evolution*, **1**.

718 Dee, D.P., Uppala, S., Simmons, A., Berrisford, P., Poli, P., Kobayashi, S., Andrae, U., Balmaseda, M.,
719 Balsamo, G. & Bauer, d.P. (2011) The ERA-Interim reanalysis: Configuration and performance
720 of the data assimilation system. *Quarterly Journal of the royal meteorological society*, **137**,
721 553-597.

722 Distler, T., Schuetz, J.G., Velásquez-Tibatá, J. & Langham, G.M. (2015) Stacked species distribution
723 models and macroecological models provide congruent projections of avian species richness
724 under climate change. *Journal of Biogeography*, **42**, 976-988.

725 Dobrowski, S.Z. (2011) A climatic basis for microrefugia: the influence of terrain on climate. *Global*
726 *Change Biology*, **17**, 1022-1035.

727 Dorrepaal, E., Aerts, R., Cornelissen, J.H., Callaghan, T.V. & Van Logtestijn, R.S. (2004) Summer
728 warming and increased winter snow cover affect *Sphagnum fuscum* growth, structure and
729 production in a sub-arctic bog. *Global Change Biology*, **10**, 93-104.

730 Elith, J. & Leathwick, J.R. (2009) Species Distribution Models: ecological explanation and prediction
731 across space and time. *Annual Review of Ecology Evolution and Systematics*, pp. 677-697.

732 Fick, S.E. & Hijmans, R.J. (2017) WorldClim 2: new 1-km spatial resolution climate surfaces for global
733 land areas. *International Journal of Climatology*, **37**, 4302-4315.

734 Fotheringham, A., Brunson, C. & Charlton, M. (2003) *Geographically weighted regression: the
735 analysis of spatially varying relationships*. John Wiley & Sons, Hoboken, USA.

736 Fox, J. & Weisberg, S. (2011) *An {R} Companion to Applied Regression, Second Edition*.

737 Geiger, R. (1950) *The climate near the ground*. Harvard University Press, Cambridge, Massachusetts,
738 USA.

739 Gillingham, P.K., Huntley, B., Kunin, W.E. & Thomas, C.D. (2012) The effect of spatial resolution on
740 projected responses to climate warming. *Diversity and Distributions*, **18**, 990-1000.

741 Gonzalez-Moreno, P., Diez, J.M., Richardson, D.M. & Vila, M. (2015) Beyond climate: disturbance
742 niche shifts in invasive species. *Global Ecology and Biogeography*, **24**, 360-370.

743 Gottfried, M., Pauli, H., Reiter, K. & Grabherr, G. (1999) A fine-scaled predictive model for changes in
744 species distribution patterns of high mountain plants induced by climate warming. *Diversity
745 and Distributions*, **5**, 241-251.

746 Graae, B.J., De Frenne, P., Kolb, A., Brunet, J., Chabrerie, O., Verheyen, K., Pepin, N., Heinken, T.,
747 Zobel, M., Shevtsova, A., Nijs, I. & Milbau, A. (2012) On the use of weather data in ecological
748 studies along altitudinal and latitudinal gradients. *Oikos*, **121**, 3-19.

749 Graae, B.J., Vandvik, V., Armbruster, W.S., Eiserhardt, W.L., Svenning, J.-C., Hylander, K., Ehrlén, J.,
750 Speed, J.D., Klanderud, K., Bråthen, K.A., Milbau, A., Opedal, O.H., Alsos, I.G., Ejrnaes, R.,
751 Bruun, H.H., Birks, H.J.B., Westergaard, K.B., Birks, H.H. & Lenoir, J. (2018) Stay or go—how
752 topographic complexity influences alpine plant population and community responses to
753 climate change. *Perspectives in Plant Ecology, Evolution and Systematics*, **30**, 41-50.

754 Greiser, C., Meineri, E., Luoto, M., Ehrlén, J. & Hylander, K. (2018) Monthly microclimate models in a
755 managed boreal forest landscape. *Agricultural and Forest Meteorology*, **250**, 147-158.

756 Guisan, A. & Thuiller, W. (2007) Predicting species distribution: offering more than simple habitat
757 models (vol 8, pg 993, 2005). *Ecology Letters*, **10**, 435-435.

758 Hannah, L., Flint, L., Syphard, A.D., Moritz, M.A., Buckley, L.B. & McCullough, I.M. (2014) Fine-grain
759 modeling of species' response to climate change: holdouts, stepping-stones, and
760 microrefugia. *Trends in Ecology & Evolution*, **29**, 390-397.

761 Haylock, M., Hofstra, N., Klein Tank, A., Klok, E., Jones, P. & New, M. (2008) A European daily high-
762 resolution gridded data set of surface temperature and precipitation for 1950–2006. *Journal
763 of Geophysical Research: Atmospheres*, **113**

764 Hijmans, R.J., Cameron, S.E., Parra, J.L., Jones, P.G. & Jarvis, A. (2005) Very high resolution
765 interpolated climate surfaces for global land areas. *International Journal of Climatology*, **25**,
766 1965-1978.

767 Holden, Z.A., Abatzoglou, J.T., Luce, C.H. & Baggett, L.S. (2011) Empirical downscaling of daily
768 minimum air temperature at very fine resolutions in complex terrain. *Agricultural and Forest
769 Meteorology*, **151**, 1066-1073.

770 Illan, J.G., Gutierrez, D. & Wilson, R.J. (2010) The contributions of topoclimate and land cover to
771 species distributions and abundance: fine-resolution tests for a mountain butterfly fauna.
772 *Global Ecology and Biogeography*, **19**, 159-173.

773 Jiménez-Valverde, A., Peterson, A.T., Soberon, J., Overton, J.M., Aragon, P. & Lobo, J.M. (2011) Use of
774 niche models in invasive species risk assessments. *Biological Invasions*, **13**, 2785-2797.

775 Jiménez-Valverde, A. (2012) Insights into the area under the receiver operating characteristic curve
776 (AUC) as a discrimination measure in species distribution modelling. *Global Ecology and
777 Biogeography*, **21**, 498-507.

778 Karger, D.N., Conrad, O., Böhner, J., Kawohl, T., Kreft, H., Soria-Auza, R.W., Zimmermann, N.E.,
779 Linder, H.P. & Kessler, M. (2017) Climatologies at high resolution for the earth's land surface
780 areas. *Scientific Data*, **4**, 170122.

781 Keppel, G., Mokany, K., Wardell-Johnson, G.W., Phillips, B.L., Welbergen, J.A. & Reside, A.E. (2015)
782 The capacity of refugia for conservation planning under climate change. *Frontiers in Ecology
783 and the Environment*, **13**, 106-112.

784 Körner, C. (2003) *Alpine plant life: functional plant ecology of high mountain ecosystems*. Springer,
785 Berlin Heidelberg, Germany.

786 Körner, C. & Hiltbrunner, E. (2018) The 90 ways to describe plant temperature. *Perspectives in Plant
787 Ecology, Evolution and Systematics*, **30**, 16-21.

788 Lembrechts, J., Nijs, I. & Lenoir, J. (2018) Incorporating microclimate into species distribution models.
789 *Ecography*,

790 Lembrechts, J.J., Milbau, A. & Nijs, I. (2014) Alien roadside species more easily invade alpine than
791 lowland plant communities in a subarctic mountain ecosystem. *PLoS One*, **9**, e89664.

792 Lembrechts, J.J., Lenoir, J., Nuñez, M.A., Pauchard, A., Geron, C., Bussé, G., Milbau, A. & Nijs, I. (2017)
793 Microclimate variability in alpine ecosystems as stepping stones for non-native plant
794 establishment above their current elevational limit. *Ecography*, **40**, 001-009.

795 Lembrechts, J.J., Pauchard, A., Lenoir, J., Nuñez, M.A., Geron, C., Ven, A., Bravo-Monasterio, P.,
796 Teneb, E., Nijs, I. & Milbau, A. (2016) Disturbance is the key to plant invasions in cold
797 environments. *Proceedings of the National Academy of Sciences of the United States of
798 America*, **113**, 14061-14066.

799 Lenoir, J., Hattab, T. & Pierre, G. (2017) Climatic microrefugia under anthropogenic climate change:
800 implications for species redistribution. *Ecography*, **40**, 253-266.

801 Lenoir, J., Graae, B.J., Aarrestad, P.A., Alsos, I.G., Armbruster, W.S., Austrheim, G., Bergendorff, C.,
802 Birks, H.J.B., Brathen, K.A., Brunet, J., Bruun, H.H., Dahlberg, C.J., Decocq, G., Diekmann, M.,
803 Dynesius, M., Ejrnaes, R., Grytnes, J.A., Hylander, K., Klanderud, K., Luoto, M., Milbau, A.,
804 Moora, M., Nygaard, B., Odland, A., Ravolainen, V.T., Reinhardt, S., Sandvik, S.M., Schei, F.H.,
805 Speed, J.D.M., Tveraabak, L.U., Vandvik, V., Velle, L.G., Virtanen, R., Zobel, M. & Svenning,
806 J.C. (2013) Local temperatures inferred from plant communities suggest strong spatial
807 buffering of climate warming across Northern Europe. *Global Change Biology*, **19**, 1470-1481.

808 Maclean, I.M.D., Suggitt, A.J., Wilson, R.J., Duffy, J.P. & Bennie, J.J. (2017) Fine-scale climate change:
809 modelling spatial variation in biologically meaningful rates of warming. *Global Change
810 Biology*, **23**, 256-268.

811 McCullough, I.M., Davis, F.W., Dingman, J.R., Flint, L.E., Flint, A.L., Serra-Diaz, J.M., Syphard, A.D.,
812 Moritz, M.A., Hannah, L. & Franklin, J. (2016) High and dry: high elevations
813 disproportionately exposed to regional climate change in Mediterranean-climate landscapes.
814 *Landscape ecology*, **31**, 1063-1075.

815 Meineri, E. & Hylander, K. (2017) Fine-grain, large-domain climate models based on climate station
816 and comprehensive topographic information improve microrefugia detection. *Ecography*, **40**,
817 1003-1013.

818 Metz, M., Rocchini, D. & Neteler, M. (2014) Surface temperatures at the continental scale: tracking
819 changes with remote sensing at unprecedented detail. *Remote Sensing*, **6**, 3822.

820 Nakagawa, S. & Schielzeth, H. (2013) A general and simple method for obtaining R² from generalized
821 linear mixed-effects models. *Methods in Ecology and Evolution*, **4**, 133-142.

822 Neteler, M., Rocchini, D., Delucchi, L. & Metz, M. (2014) Massive data processing in GRASS GIS 7: A
823 new gap-filled MODIS Land Surface Temperature time series data set. *FOSS4G-Europe 2014*
824 (ed by).

825 Neteler, M., Metz, M., Rocchini, D., Rizzoli, A., Flacio, E., Engeler, L., Guidi, V., Lüthy, P. & Tonolla, M.
826 (2013) Is Switzerland suitable for the invasion of *Aedes albopictus*? *PLoS One*, **8**, e82090.

827 Niittynen, P. & Luoto, M. (2017) The importance of snow in species distribution models of arctic
828 vegetation. *Ecography*,

829 Opedal, O.H., Armbruster, W.S. & Graae, B.J. (2015) Linking small-scale topography with
830 microclimate, plant species diversity and intra-specific trait variation in an alpine landscape.
831 *Plant Ecology & Diversity*, **8**, 305-315.

832 Pauchard, A., Kueffer, C., Dietz, H., Daehler, C.C., Alexander, J., Edwards, P.J., Arévalo, J.R., Cavieres,
833 L.A., Guisan, A., Haider, S., Jakobs, G., McDougall, K., Millar, C.I., Naylor, B.J., Parks, C.G., Rew,
834 L.J. & Seipel, T. (2009) Ain't no mountain high enough: plant invasions reaching new
835 elevations. *Frontiers in Ecology and the Environment*, **7**, 479-486.

836 Pauli, J.N., Zuckerberg, B., Whiteman, J.P. & Porter, W. (2013) The subnivium: a deteriorating
837 seasonal refugium. *Frontiers in Ecology and the Environment*, **11**, 260-267.

838 Poorter, H., Fiorani, F., Pieruschka, R., Wojciechowski, T., van der Putten, W.H., Kleyer, M., Schurr, U.
839 & Postma, J. (2016) Pampered inside, pestered outside? Differences and similarities between
840 plants growing in controlled conditions and in the field. *New Phytologist*, **212**, 838-855.

841 Potter, K.A., Woods, H.A. & Pincebourde, S. (2013) Microclimatic challenges in global change biology.
842 *Global Change Biology*, **19**, 2932-2939.

843 Pottier, J., Malenovský, Z., Psomas, A., Homolová, L., Schaepman, M.E., Choler, P., Thuiller, W.,
844 Guisan, A. & Zimmermann, N.E. (2014) Modelling plant species distribution in alpine
845 grasslands using airborne imaging spectroscopy. *Biology letters*, **10**, 20140347.

846 Pradervand, J.-N., Dubuis, A., Pellissier, L., Guisan, A. & Randin, C. (2014) Very high resolution
847 environmental predictors in species distribution models: Moving beyond topography?
848 *Progress in Physical Geography*, **38**, 79-96.

849 R Core Team (2015) *R: a language and environment for statistical computing*. R Foundation for
850 Statistical Computing.

851 Randin, C.F., Vuissoz, G., Liston, G.E., Vittoz, P. & Guisan, A. (2009a) Introduction of snow and
852 geomorphic disturbance variables into predictive models of alpine plant distribution in the
853 Western Swiss Alps. *Arctic, Antarctic, and Alpine Research*, **41**, 347-361.

854 Randin, C.F., Engler, R., Normand, S., Zappa, M., Zimmermann, N.E., Pearman, P.B., Vittoz, P.,
855 Thuiller, W. & Guisan, A. (2009b) Climate change and plant distribution: local models predict
856 high-elevation persistence. *Global Change Biology*, **15**, 1557-1569.

857 Rebaudo, F., Faye, E. & Dangles, O. (2016) Microclimate data improve predictions of insect
858 abundance models based on calibrated spatiotemporal temperatures. *Frontiers in*
859 *Physiology*, **7**, 139.

860 Scherrer, D. & Körner, C. (2011) Topographically controlled thermal-habitat differentiation buffers
861 alpine plant diversity against climate warming. *Journal of Biogeography*, **38**, 406-416.

862 Sears, M.W., Raskin, E. & Angilletta, M.J. (2011) The world is not flat: defining relevant thermal
863 landscapes in the context of climate change. *Integrative and Comparative Biology*, **51**, 666-
864 675.

865 Shanks, R.E. (1956) Altitudinal and microclimatic relationships of soil temperature under natural
866 vegetation. *Ecology*, **37**, 1-7.

867 Sing, T., Sander, O., Beerenwinkel, N. & Lengauer, T. (2005) ROCr: visualizing classifier performance
868 in R. *Bioinformatics*, **21**, 7781.

869 Slavich, E., Warton, D.I., Ashcroft, M.B., Gollan, J.R. & Ramp, D. (2014) Topoclimate versus
870 macroclimate: how does climate mapping methodology affect species distribution models
871 and climate change projections? *Diversity and Distributions*, **20**, 952-963.

872 Stewart, L., Simonsen, C.E., Svenning, J.C., Schmidt, N.M. & Pellissier, L. (2018) Forecasted
873 homogenization of high Arctic vegetation communities under climate change. *Journal of*
874 *biogeography*, **45**, 2576-2587.

875 Su, Y.F., Foody, G.M. & Cheng, K.S. (2012) Spatial non-stationarity in the relationships between land
876 cover and surface temperature in an urban heat island and its impacts on thermally sensitive
877 populations. *Landscape and Urban Planning*, **107**, 172-180.

878 Thompson, K.L., Zuckerberg, B., Porter, W.P. & Pauli, J.N. (2018) The phenology of the subnivium.
879 *Environmental Research Letters*, **13**, 064037.

- 880 Wan, Z., Hook, S. & Hulley, G. (2015) MOD11C2 MODIS/Terra Land Surface Temperature/Emissivity
881 8-Day L3 Global 0.05Deg CMG V006 [Data set]. In, NASA EOSDIS LP DAAC.
- 882 Wan, Z.M. (2008) New refinements and validation of the MODIS Land-Surface
883 Temperature/Emissivity products. *Remote Sensing of Environment*, **112**, 59-74.
- 884 Warren, D.L., Glor, R.E. & Turelli, M. (2008) Environmental niche equivalency versus conservatism:
885 quantitative approaches to niche evolution. *Evolution*, **62**, 2868-2883.
- 886 Wason, J.W., Bevilacqua, E. & Dovciak, M. (2017) Climates on the move: Implications of climate
887 warming for species distributions in mountains of the northeastern United States.
888 *Agricultural and Forest Meteorology*, **246**, 272-280.
- 889 Wild, J., Kopecký, M., Macek, M., Šanda, M., Jankovec, J. & Haase, T. (2019) Climate at ecologically
890 relevant scales: A new temperature and soil moisture logger for long-term microclimate
891 measurement. *Agricultural and Forest Meteorology*, **268**, 40-47.
- 892 Williams, C.M., Henry, H.A.L. & Sinclair, B.J. (2015) Cold truths: how winter drives responses of
893 terrestrial organisms to climate change. *Biological Reviews*, **90**, 214-235.
- 894 Willis, K.J. & Bhagwat, S.A. (2009) Biodiversity and climate change. *Science*, **326**, 806-807.
- 895 Wood, S. (2006) *Generalized Additive Models: An introduction with R*. Chapman and Hall/CRC.
- 896 Wundram, D., Pape, R. & Löffler, J. (2010) Alpine soil temperature variability at multiple scales. *Arctic*
897 *Antarctic and Alpine Research*, **42**, 117-128.
- 898 Yannic, G., Pellissier, L., Le Corre, M., Dussault, C., Bernatchez, L. & Côté, S.D. (2014) Temporally
899 dynamic habitat suitability predicts genetic relatedness among caribou. *Proceedings of the*
900 *Royal Society of London B: Biological Sciences*, **281**, 20140502.
- 901 Zellweger, F., De Frenne, P., Lenoir, J., Rocchini, D. & Coomes, D. (2019) Advances in microclimate
902 ecology arising from remote sensing. *Trends in ecology & evolution*,
- 903 Zhang, T. (2005) Influence of the seasonal snow cover on the ground thermal regime: An overview.
904 *Reviews of Geophysics*, **43**
- 905 Zuur, A.F., Ieno, E.N., Walker, N.J., Saveliev, A.A. & Smith, G.M. (2009) *Mixed effects models and*
906 *extensions in ecology with R*. Springer, New York, USA.

907

908 **Data Accessibility Statement**

909 Most used climate datasets are freely available (see Methods section). In-situ soil temperature
910 and species distribution data will be published in an open access data repository.

911 **Tables**

912 *Table 1: The eight studied climate datasets and their geographical and temporal extent, spatial resolution and measurement focus.*

Dataset	Initial source	Geographical extent	Spatial resolution	Measurement focus	Temporal coverage
a) WorldClim	WorldClim	Global	30''	Free-air	1970-2000
b) CHELSA	CHELSA	Global	30''	Free-air	1979-2013
c) Downscaled	CHELSA	10000 km ²	1''	Free-air	1979-2013
d) Topoclimate	Aalto et al. (2018)	10000 km ²	1''	Free-air	1981-2010
e) MODIS LST	MODIS	Global	30''	Surface	2015-2017
f) EuroLST	MODIS	Europe	~7.5''	Surface	2001-2011
g) E-OBS	E-OBS	Europe	0.1°	Free-air	2015-2017
h) Soil temperature	iButtons	10000 km ²	1''	Soil	2015-2017

913

914 **Table 2: Overview of in-situ soil temperature measurement plots in Sweden and Norway (n=106).** For each gradient (numbers from 1) to 4)
 915 refer to the map in Fig. 1), we present the number of elevation gradients (i.e. different mountains monitored), sites and plots (with more plots
 916 than sites indicating repeated temperature measurements in a $< 20 \times 20$ m area), as well as the temporal extent, the length of the elevation
 917 gradient, and if species data is available to run species distribution models (SDMs).

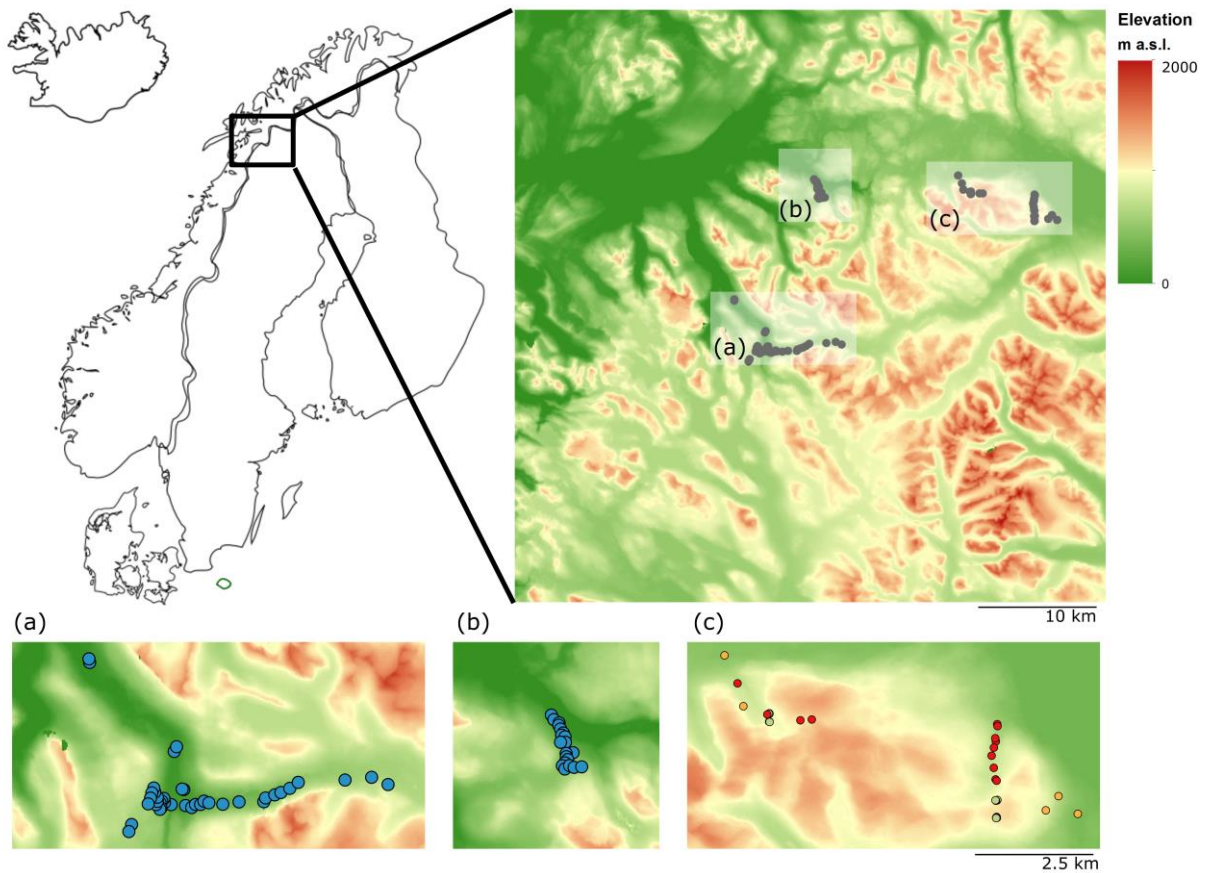
Region	#	of Sites	Plots	Surface area	Temporal extent	Elevation (m a.s.l.)	Species data
		gradients					
1) Norway	3	59	59	2×100 m	01/08/15-31/07/17	0-700	Yes
2) Sweden	2	4	23	0.6×1.2 m	01/08/15-31/07/16	900-1100	No
3) Sweden	2	6	11	0.6×1.2 m	01/08/16-31/07/17	400-900	No
4) Sweden	2	13	13	2×10 m	01/08/16-31/07/17	400-1200	No

918

919 **Table 3: Differences in average temperature between the climatic datasets.** Two-by-two
920 comparisons between the three studied bioclimatic variables (*Bio1* = mean annual
921 temperature, *Bio10* = mean temperature of the warmest quarter, *Bio11* = mean temperature
922 of the coldest quarter) for the different climatic datasets (except WorldClim) after correcting
923 for inter-annual and climate change effects using ERA Interim (see methods for details).
924 Analysis based on data from all 106 measurement locations, for MODIS LST, E-OBS and in-
925 situ soil temperature, only the data from 2016-2017 is tested. Values show the differences in
926 average temperature in °C between the two datasets, with positive values indicating higher
927 temperatures in the variable in the column than in the row. Values in bold are significant at
928 $p < 0.05$ from paired *t*-tests. Relationships with in-situ soil temperature are visualised in Fig.
929 S1, while some relationships among the other variables are visualised in Fig. S2.

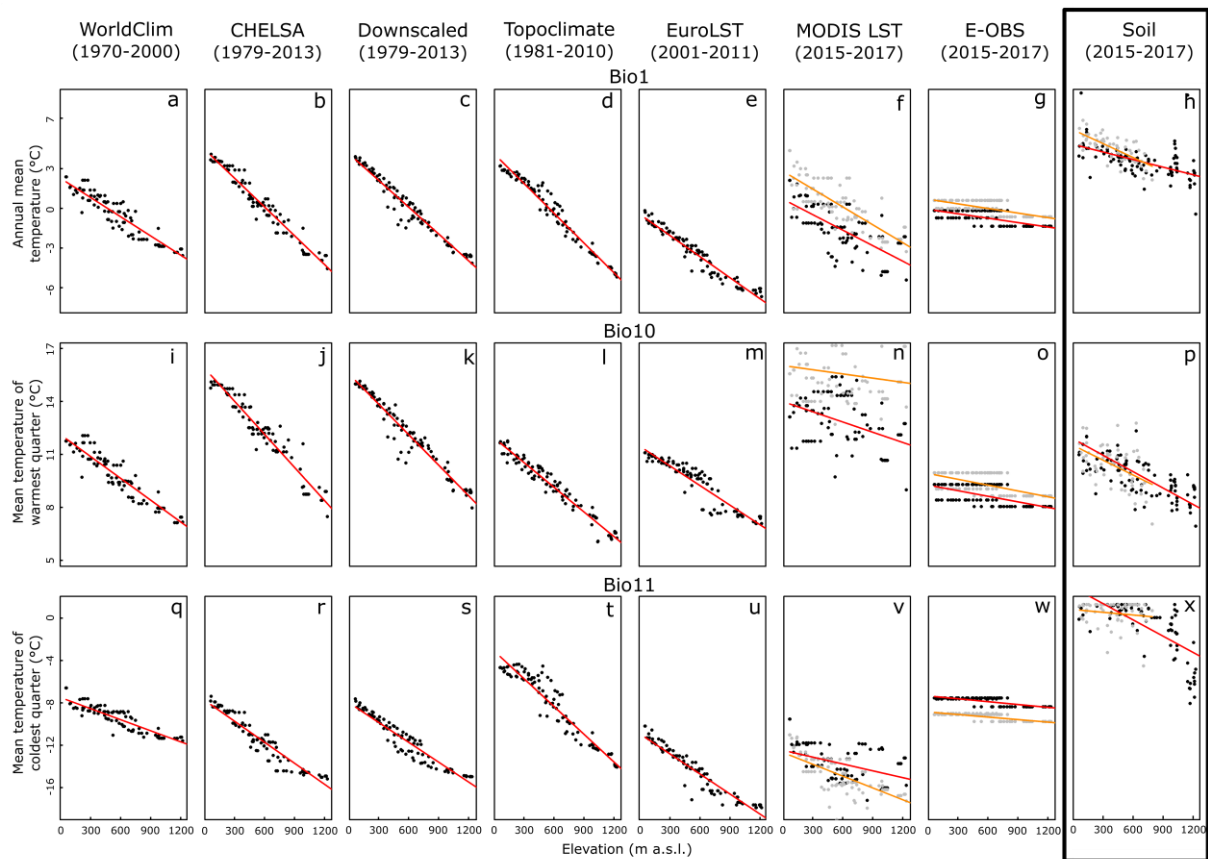
	<i>CHELSA</i> <i>down</i>	<i>Topo-</i> <i>climate</i>	<i>EuroLST</i>	<i>MODIS</i> <i>LST</i>	<i>E-OBS</i>	<i>In-situ</i> <i>soil</i>
Bio1						
<i>CHELSA</i>	-0.03	-0.36	-3.19	-1.96	-1.11	2.67
<i>CHELSA down</i>	-	-0.33	-3.16	-1.92	-1.08	2.68
<i>Topoclimate</i>	-	-	-2.84	-1.59	-0.75	3.00
<i>EuroLST</i>	-	-	-	1.22	2.08	5.77
<i>MODIS LST</i>	-	-	-	-	0.91	4.53
<i>E-OBS</i>	-	-	-	-	-	3.53
Bio10						
<i>CHELSA</i>	-0.03	-2.86	-3.28	1.45	-2.85	-1.48
<i>CHELSA down</i>	-	-2.83	-3.25	1.49	-2.81	-1.48
<i>Topoclimate</i>	-	-	-0.42	4.30	0.01	1.24
<i>EuroLST</i>	-	-	-	4.70	0.43	1.67
<i>MODIS LST</i>	-	-	-	-	-4.23	-3.15
<i>E-OBS</i>	-	-	-	-	-	1.12
Bio11						
<i>CHELSA</i>	-0.03	2.60	-2.47	-4.82	0.02	6.30
<i>CHELSA down</i>	-	2.63	-2.44	-4.78	0.05	6.29
<i>Topoclimate</i>	-	-	-5.07	-7.39	-2.58	3.74
<i>EuroLST</i>	-	-	-	-2.35	2.49	8.72
<i>MODIS LST</i>	-	-	-	-	4.89	10.99
<i>E-OBS</i>	-	-	-	-	-	6.06

930



932

933 **Figure 1: Study area and measurement locations.** Location of the study area in Scandinavia
 934 (left) and digital elevation model (DEM) at 1 arc-second resolution (ca. 30 x 30 m at the
 935 equator) across the study area (right). Dots on the DEM show locations of the 106 soil
 936 temperature measurements. Species data sampling was done in the locations marked with
 937 blue dots (a and b). See Table 2 for datasets: blue = 1), orange = 2), green = 3), red = 4).
 938 Elevational gradients ranging from 0 till 700 m a.s.l. (a and b) and from 400 to 1200 m a.s.l.
 939 (c).



940

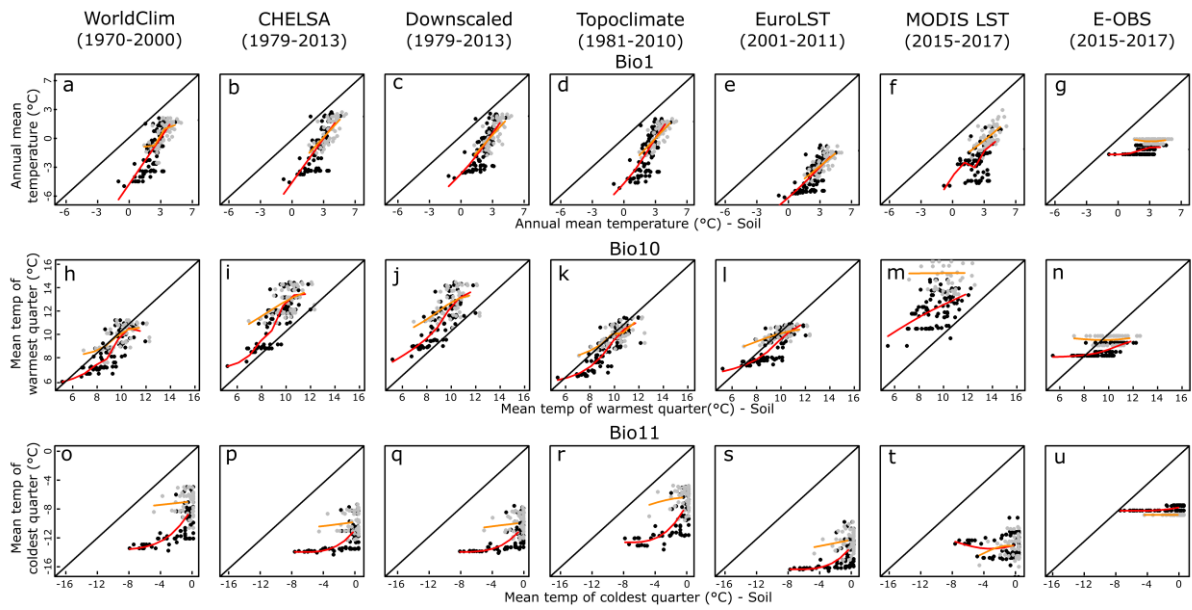
941 **Figure 2: Temperature patterns against elevation for the different temperature data sets.**

942 *Average annual (Bio1, a-h), summer (Bio10, i-p) and winter (Bio11, q-x) temperature for the*

943 *eight climate datasets (columns, temporal extent between brackets) against elevation of the*

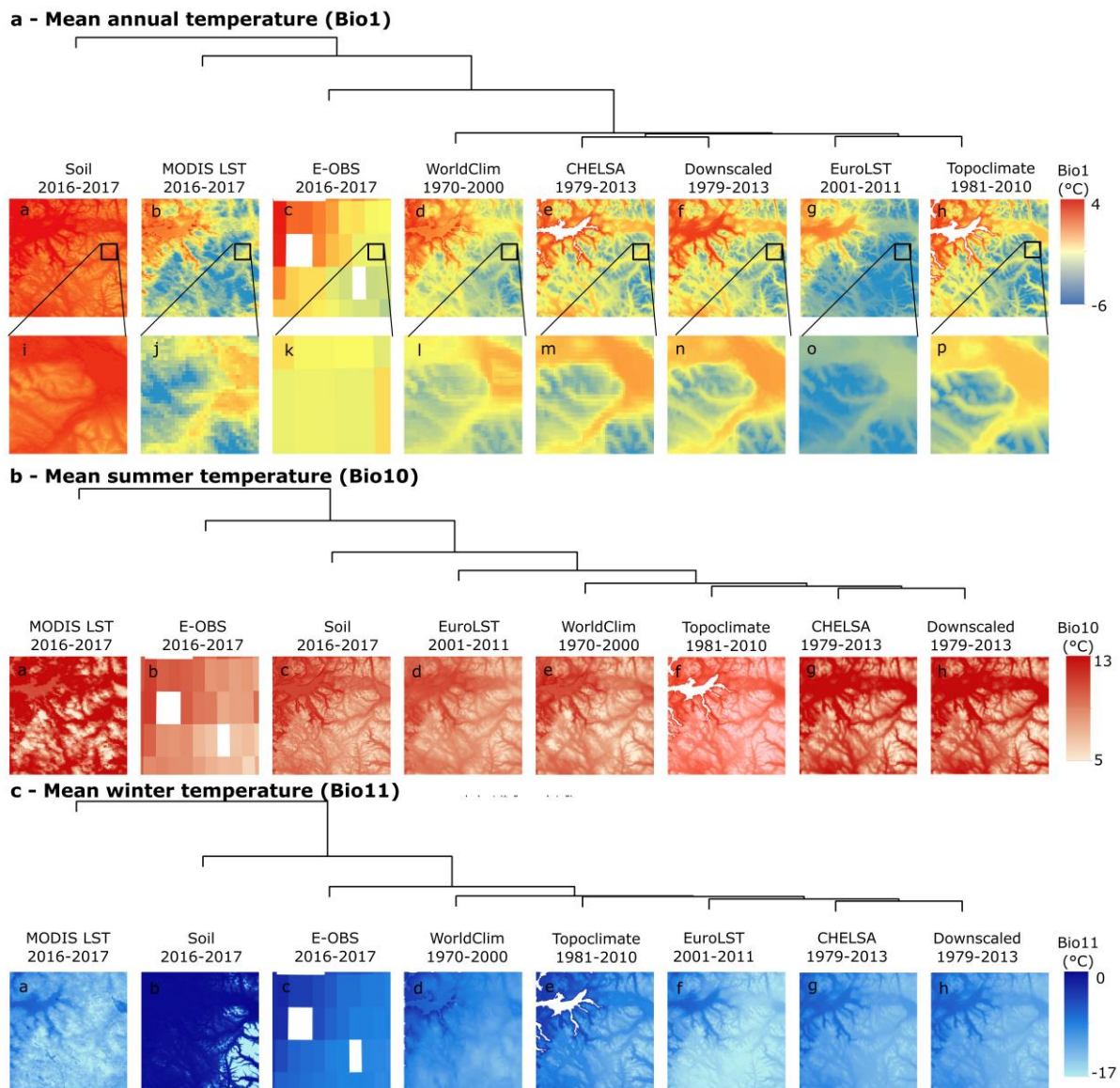
944 *106 measurement locations. Orange (2015-2016) and red (2016-2017) lines are fitted with*

945 *linear models.*



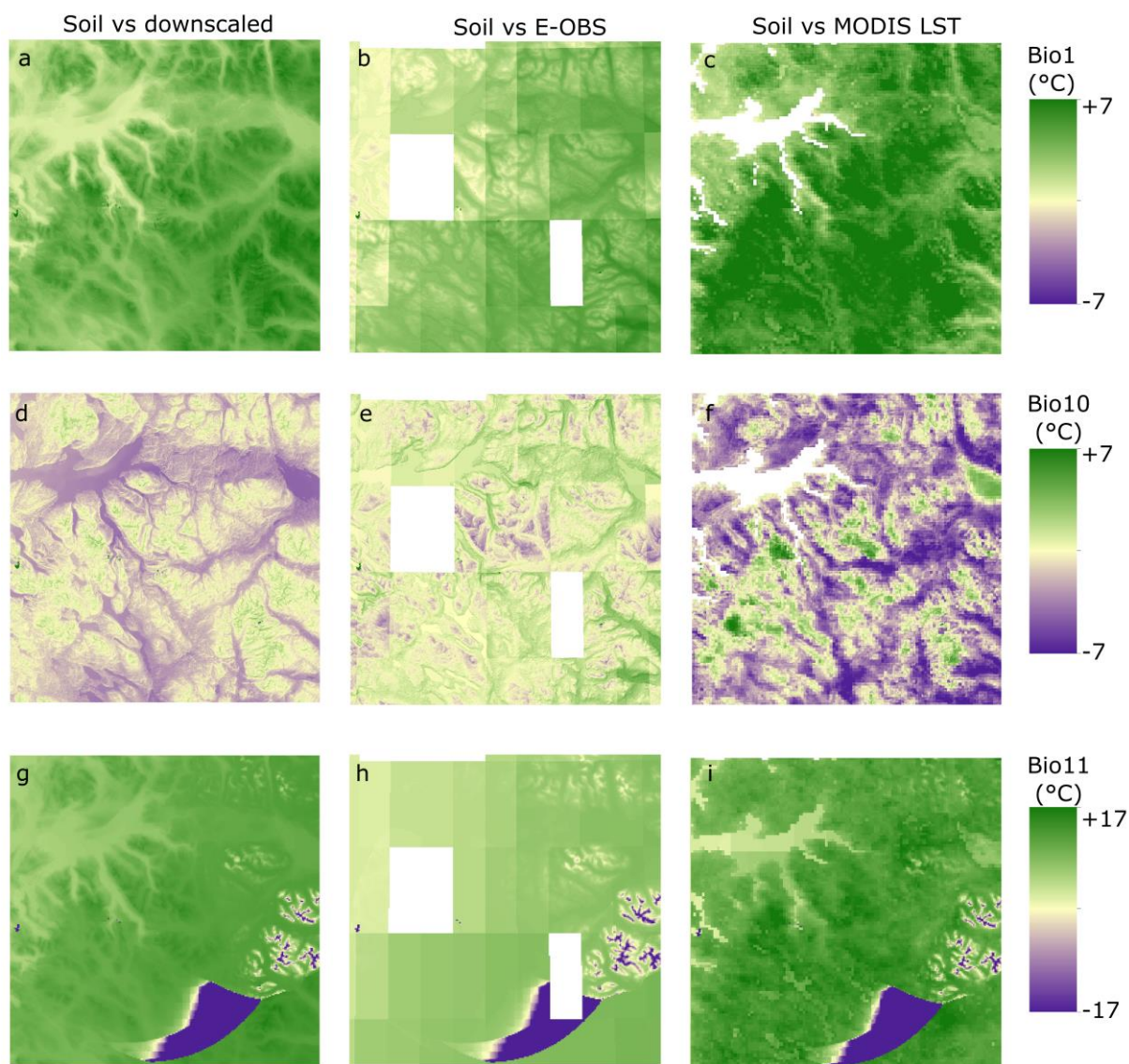
946

947 **Figure 3: Plot-by-plot comparisons of soil temperature data against 7 other sources of**
 948 **temperature data. Mean annual (Bio1, a-g), summer (Bio10, h-n) and winter (Bio11, o-u)**
 949 **temperature, for all 106 measurement locations for 2015-2016 (orange lines, grey dots) and**
 950 **2016-2017 (red lines, black dots). Black lines show first bisectors (a hypothetical perfect**
 951 **match), red and orange lines are fitted with generalised additive models for each year of**
 952 **temperature measurements separately. Measurement periods between brackets.**



953

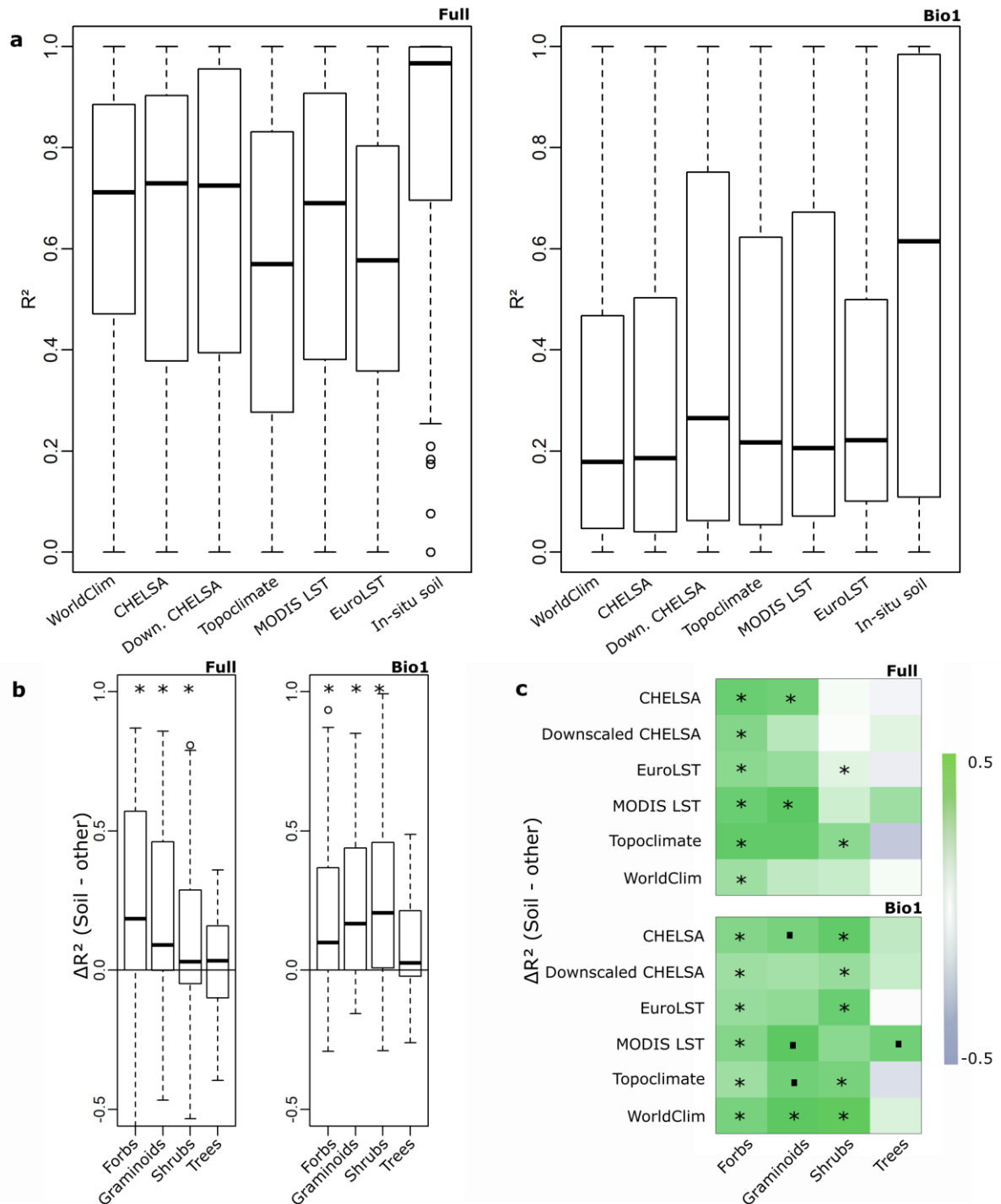
954 **Figure 4: Dendrograms of collinearity between different temperature datasets.** Data from
 955 the 106 measurement locations for mean annual (a - Bio1), summer (b – Bio10) and winter (c
 956 – Bio11) temperature. Measurement periods between brackets. Maps show the regional (100
 957 × 100 km) predictions for each dataset and bioclimatic variable. For Bio1, cut-outs of the
 958 maps are shown (location specified by black squares).



959

960 **Figure 5: Differences (in °C) between regionally modelled soil temperature and other**
 961 **temperature data sources. Differences in annual average temperature (Bio1), mean**
 962 **temperature of the warmest quarter (Bio10) and mean temperature of the coldest quarter**
 963 **(Bio11) are shown for soil temperature versus downscaled CHELSA (left), E-OBS (middle)**
 964 **and MODIS LST (right). Comparisons between soil temperature and CHELSA, WorldClim**
 965 **and EuroLST are not shown, as trends were similar. Values below zero indicate a lower value**
 966 **for the soil temperature compared with the other dataset; values above zero a higher value.**

967



968

969 **Figure 6: Proportion of explained variance (marginal R^2) by species distribution models**

970 **(SDMs) using the different temperature datasets. (a) Boxplots of the marginal R^2 of**

971 **distribution models for 50 plant species in a subset of 59 plots, based on binomial GLMMs**

972 **built with the different temperature datasets: using Bio1, 10 and 11 together (left, 'Full') or**

973 **Bio1 only (right, 'Bio1'). (b) Differences in marginal R^2 between the models using soil**

974 *temperature and all other datasets for forbs (N = 25), graminoids (N = 7), (dwarf) shrubs (N*
975 *= 15) and trees (N = 3). (c) Heatmaps visualising the differences in marginal R² between the*
976 *models using soil temperature and each of the other climatic datasets for the different growth*
977 *forms. Green (positive values) indicates better performance of soil temperature models, blue*
978 *a better performance of the other dataset in question. “*” and “.” respectively indicate*
979 *significant ($p < 0.05$) and marginally significant ($0.05 < p < 0.1$) differences from zero as*
980 *obtained with a two-sided t-test.*

981

982

983